

Summary

The Skellefte district is a Paleoproterozoic, mainly metavolcanic region in northern Sweden, and one of the richest metallogenic provinces in the country. Many geological and geophysical investigations have been performed to help design exploration strategies for targets at depths below 1km. We are focussing on the Kristineberg mining area to the west of the Skellefte District. The area has been subject to several stages of deformation, the lithologies of interest are covered by massive sheet-like intrusions and outcrops are rare. Hence, the geological setting is not yet clearly understood and the existing 3D models carry large uncertainties. We are performing geologically constrained joint inversions using regional gravity, magnetic and magnetotelluric data. Petrophysical information is available to help develop joint coupling approaches but there are still many practical questions regarding how best to integrate the data via inversion.

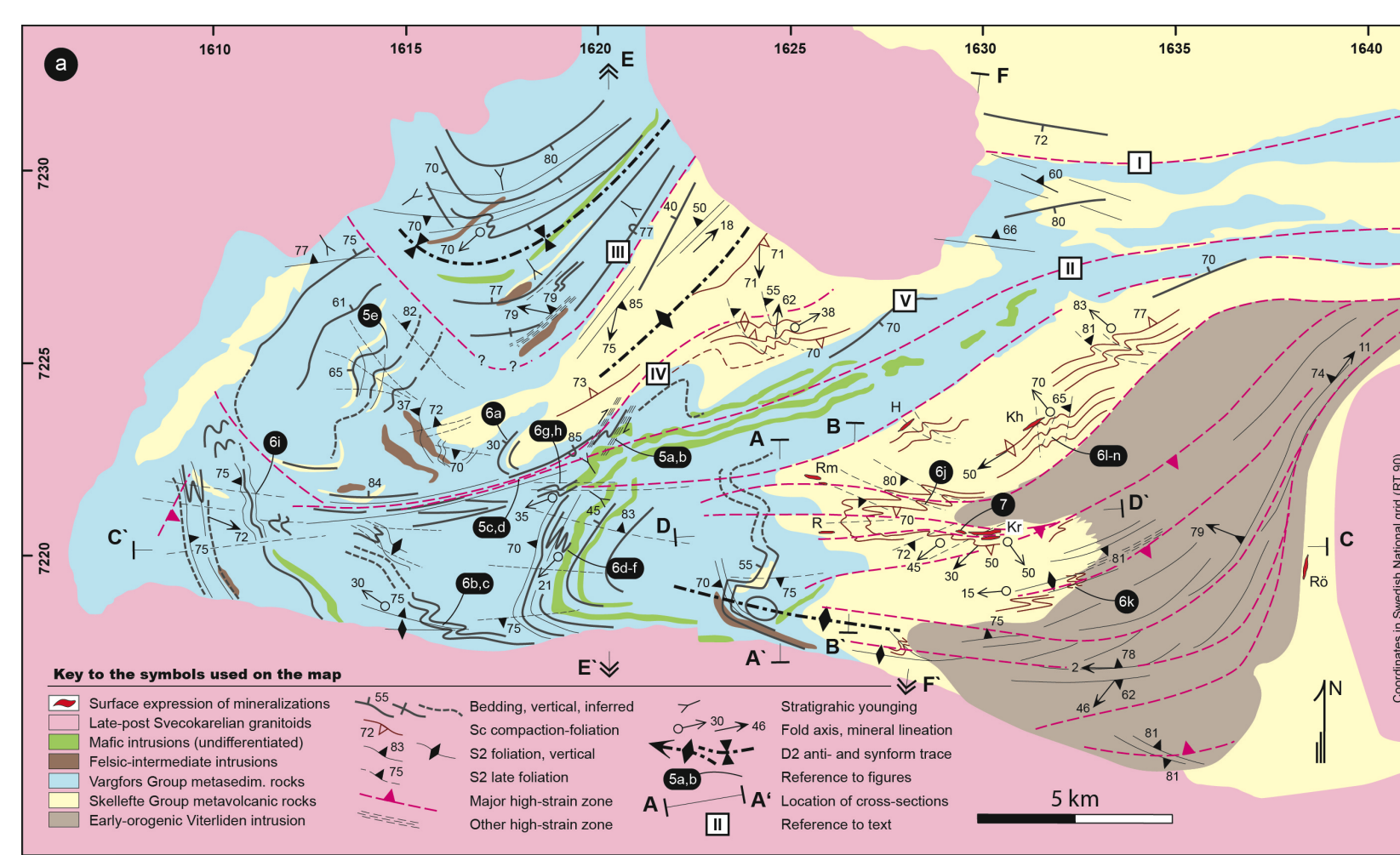


Figure 1 : Geological map of the Kristineberg area [1].

Data processing

We removed a linear trend from the gravity data, and a regional component from both the gravity and magnetic data following the approach of [2]. We transformed total field magnetic data into magnetic amplitude data (not shown) using a similar approach as [2].

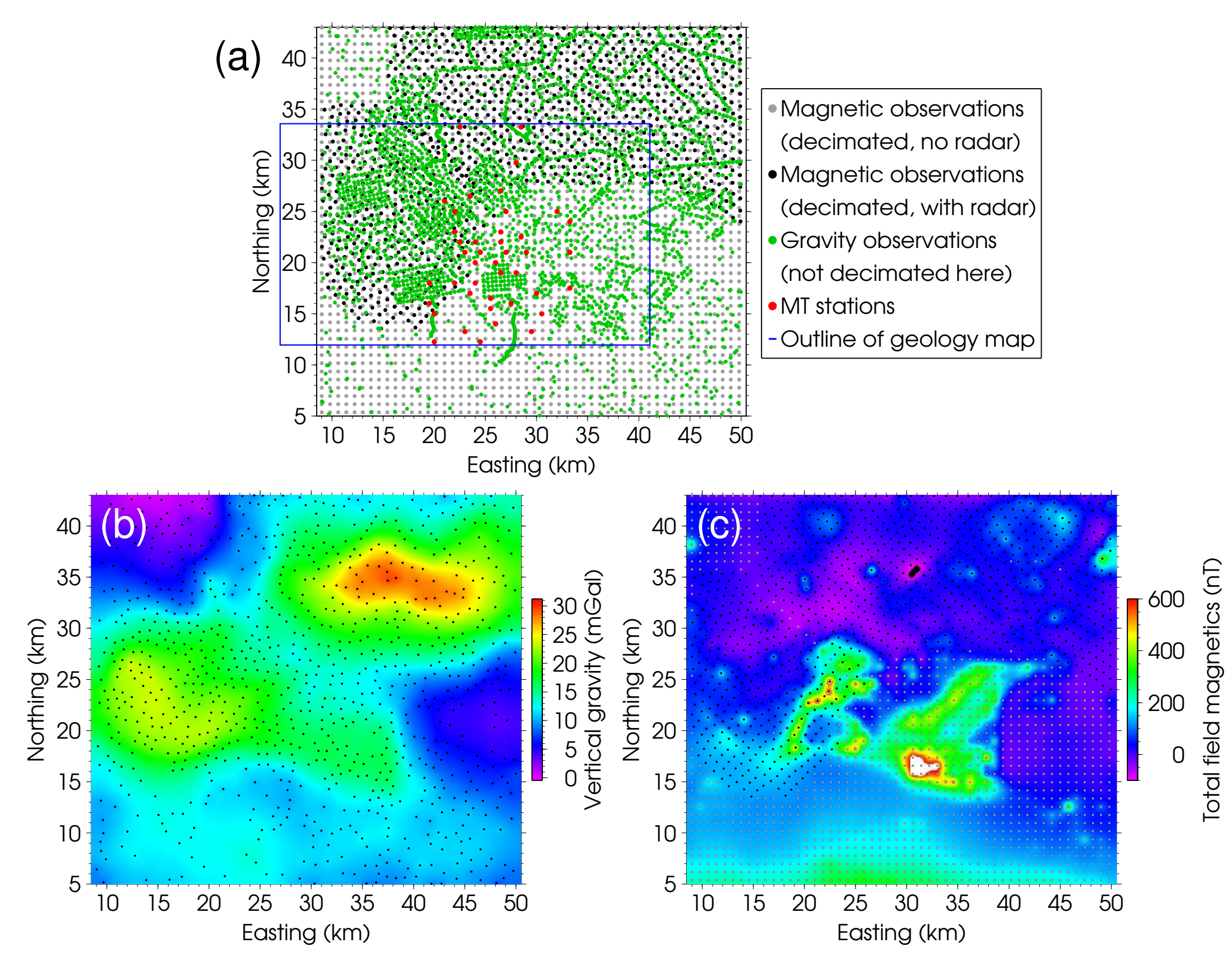


Figure 2 : (a) Data observation locations, (b) gravity response after regional removal (decimated here), (c) magnetic response after regional removal. Coordinates are in our own system.

Independent inversion

We inverted the gravity and magnetic total field data using the methods of [3] (see Figs. 3 through 5); the magnetic amplitude data using the approach of [4]; and the MT data were inverted using the methods of [5] (see Fig. 6). The recovered magnetic susceptibility models from inversion of total field data (Figs. 4 and 5) and magnetic amplitude data (not shown) displayed minor differences only below the older felsic Viterliden Intrusion (see Fig. 1) where petrophysical measurements suggest significant levels of remanence. However, the data available in that region do not include radar (see Fig. 2a) and cannot be located vertically beyond an approximated average flight height, requiring that large uncertainties be assigned. Modelling errors from the assumption of no remanence are expected to be below that uncertainty threshold so we used total field data rather than magnetic amplitude data in our subsequent inversions. The recovered magnetic susceptibility model with default depth weighting (Fig. 4) has material pushed away from the surface, which is inconsistent with knowledge of the geology. Hence, we performed subsequent magnetic inversions with reduced depth weighting (Fig. 5).

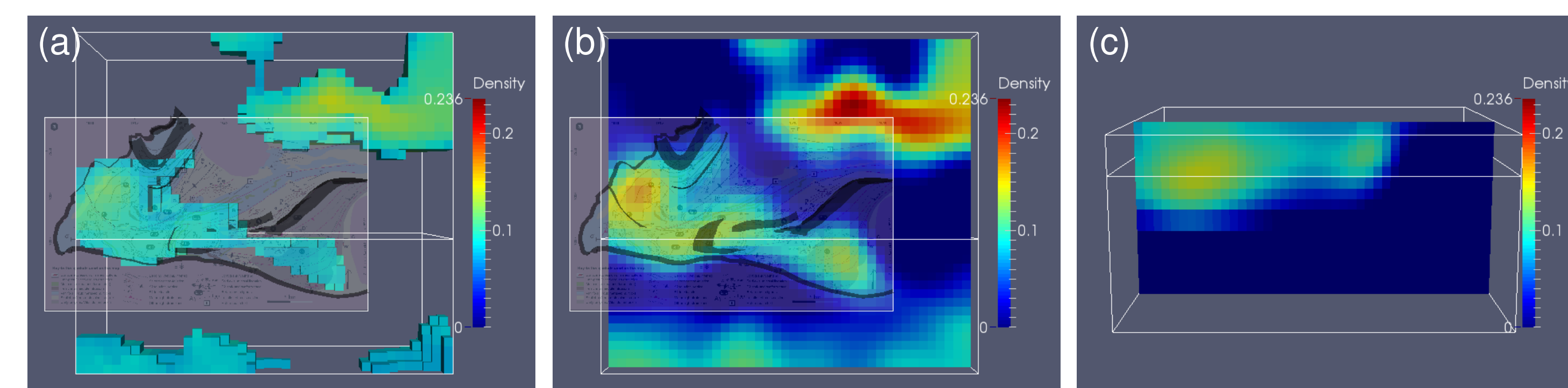


Figure 3 : Density model (g/cc) from independent inversion: (a) top view of 0.07 threshold, (b) top view of -4km depth slice, (c) side view looking north of northing = 20km slice. Panels (a) and (b) include opaque interpreted surfaces (black) and geological map.

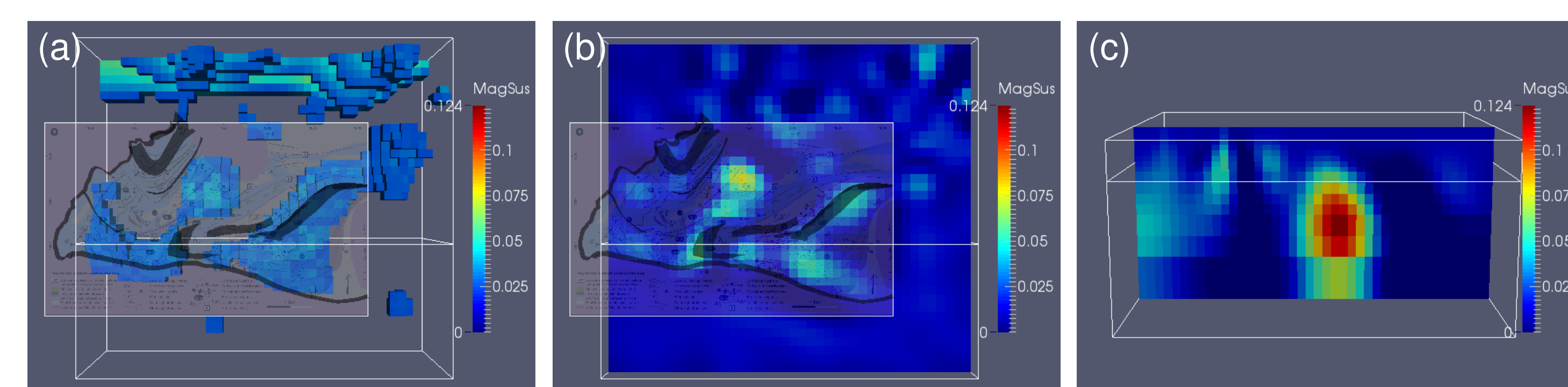


Figure 4 : Magnetic susceptibility model (SI) from independent inversion with default depth weighting: (a) top view of 0.025 threshold, (b) and (c) as for Fig. 3.

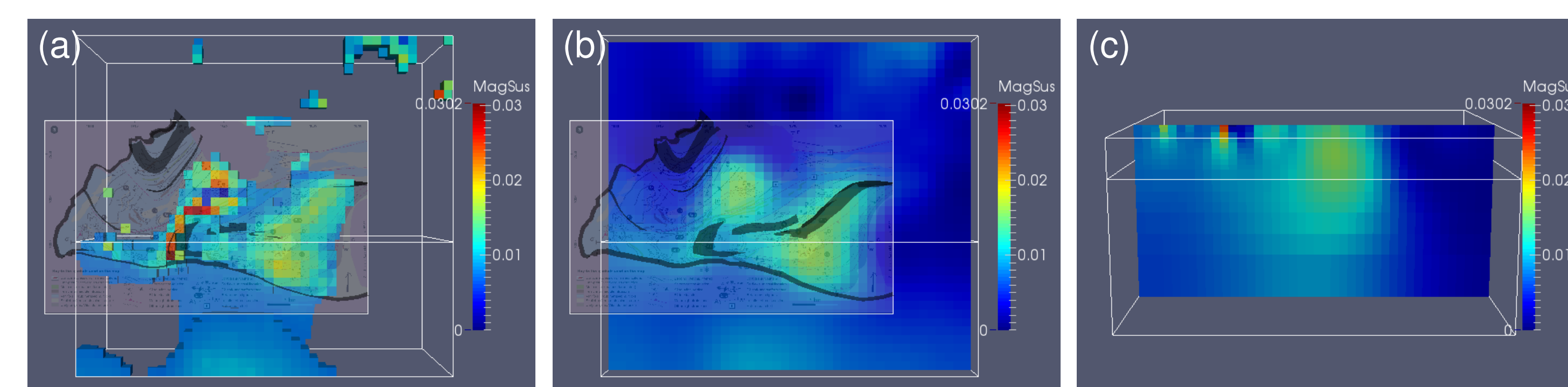


Figure 5 : Magnetic susceptibility model (SI) from independent inversion with reduced depth weighting: (a) top view of 0.007 threshold, (b) and (c) as for Fig. 3.

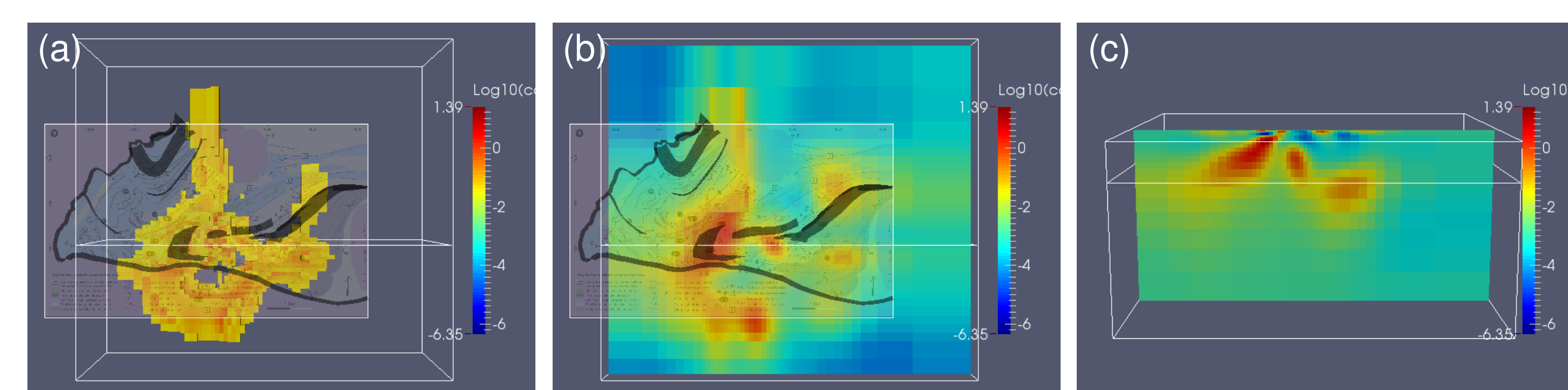


Figure 6 : Conductivity model (\log_{10} S/m) from independent inversion, from the work of [6]: (a) top view of -1.5 threshold, (b) and (c) as for Fig. 3.

Joint inversion with petrophysical coupling

Using the methods of [7], we performed a joint (simultaneous) inversion, encouraging a linear trend consistent with the petrophysical data from the Kristineberg area (Fig. 7). However, that linear trend fails to accommodate much higher susceptibility values recovered at depth and the inversion was not able to provide an appropriate result (Fig. 9). To reduce the susceptibility values, the inversion moved deeper material to the surface. Using implicit linear coupling (again, see [7]) showed moderate improvement (Fig. 10). The recovered density models did not change significantly from the independent results so are not shown.

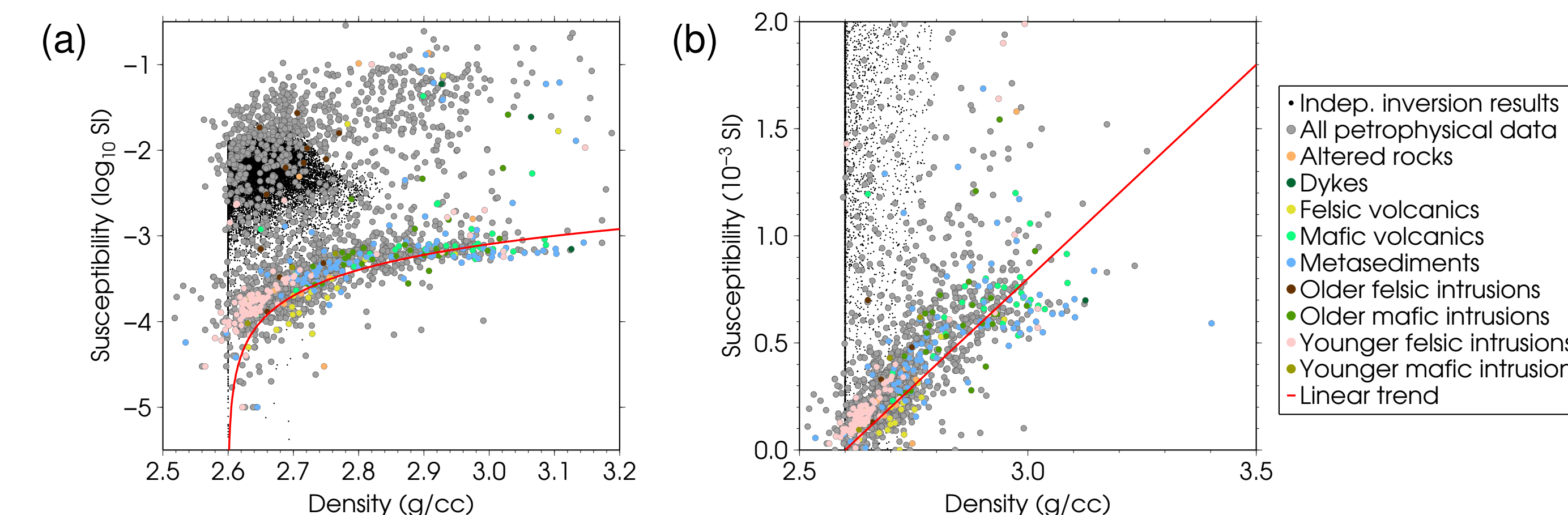


Figure 7 : Petrophysical information available for the Kristineberg area (various colours), all petrophysical information for the Skellefte district (grey), and recovered model values from the independent inversions (black). The red line shows the linear trend used in the joint inversion with petrophysical coupling (Fig. 9). Panel (a) has \log_{10} scale for susceptibility whereas panel (b) has linear scale and only shows a portion of the full range of data.

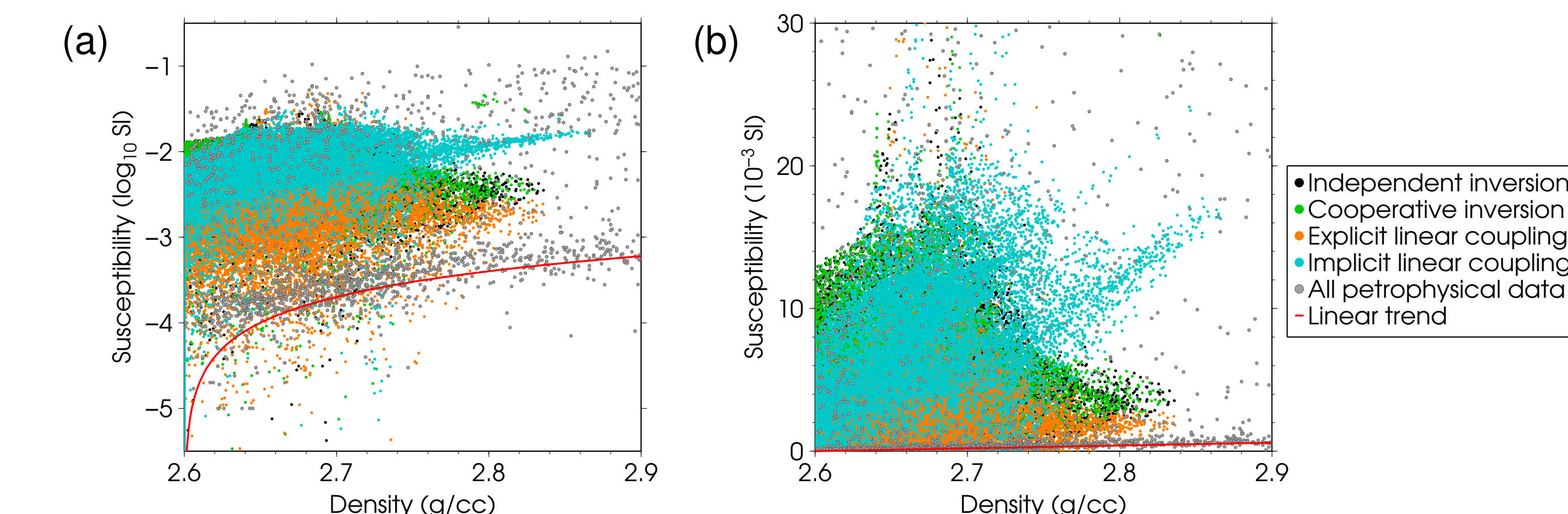


Figure 8 : Density versus susceptibility scatter plots for models recovered from various inversions. The red line shows the linear trend used in the joint inversion with petrophysical coupling (Fig. 9). Panel (a) has \log_{10} scale for susceptibility whereas panel (b) has linear scale. The vertical axes in both panels do not cover all recovered values: some of the lowest susceptibility values are not plotted in (a) and some of the highest values are not plotted in (b).

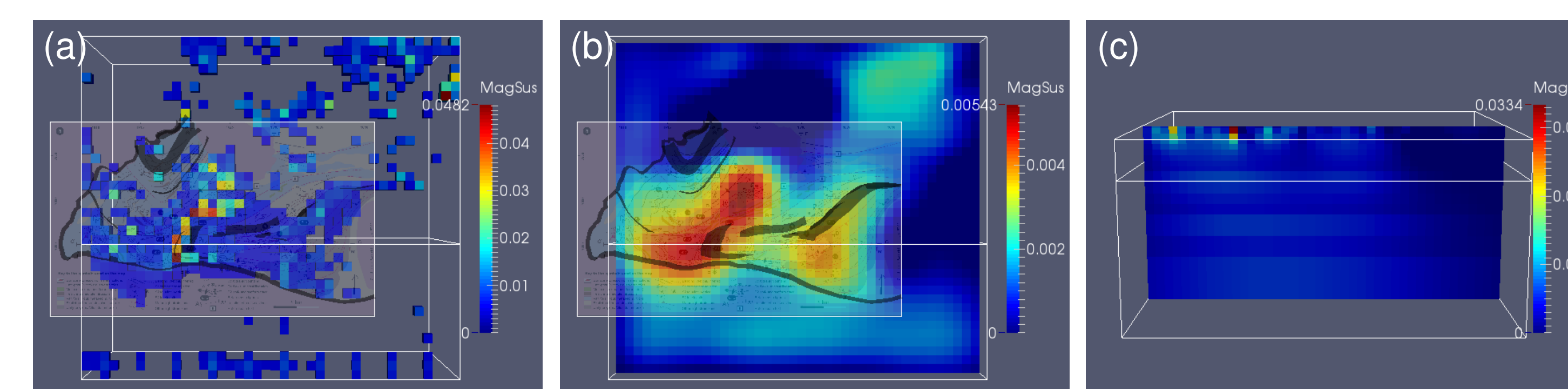


Figure 9 : Magnetic susceptibility model (SI) from joint inversion with explicit linear coupling and reduced depth weighting: (a) top view of 0.005 threshold, (b) and (c) as for Fig. 3. The upper colour-scale limits in (b) and (c) have been changed to accentuate the recovered features.

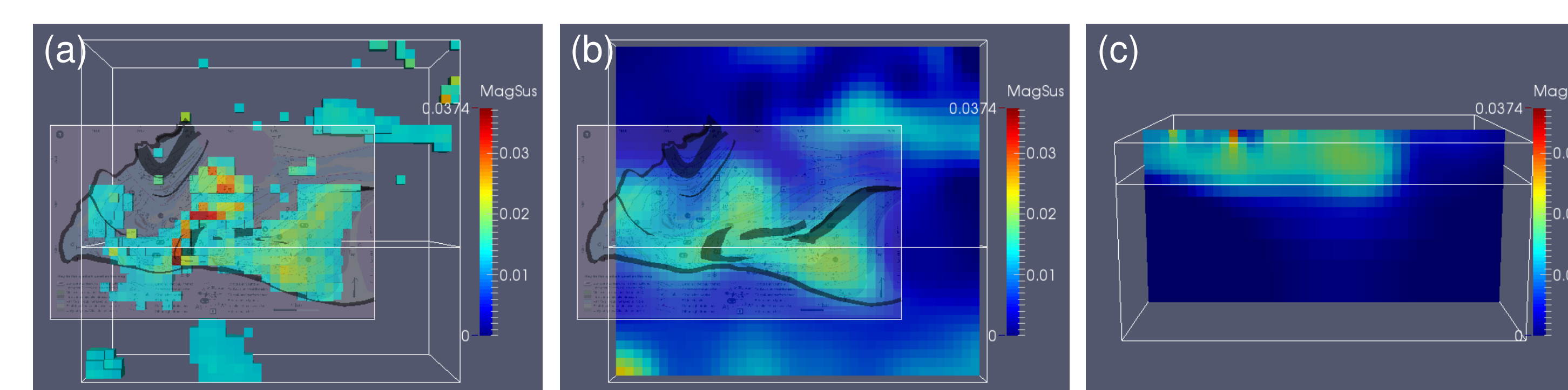


Figure 10 : Magnetic susceptibility model (SI) from joint inversion with implicit linear coupling and reduced depth weighting: (a) top view of 0.0125 threshold, (b) and (c) as for Fig. 3.

Cooperative inversion with structural coupling

We performed a cooperative (sequential) inversion following the methods of [8]. This approach promotes structural similarity by altering the smoothness weights iteratively from one recovered model to another. We began with the independent gravity inversion result and iterated for 10 inversions of each dataset. This cooperative procedure converged well but does not present any significant improvement over the independent results and has generated some spurious small artifacts.

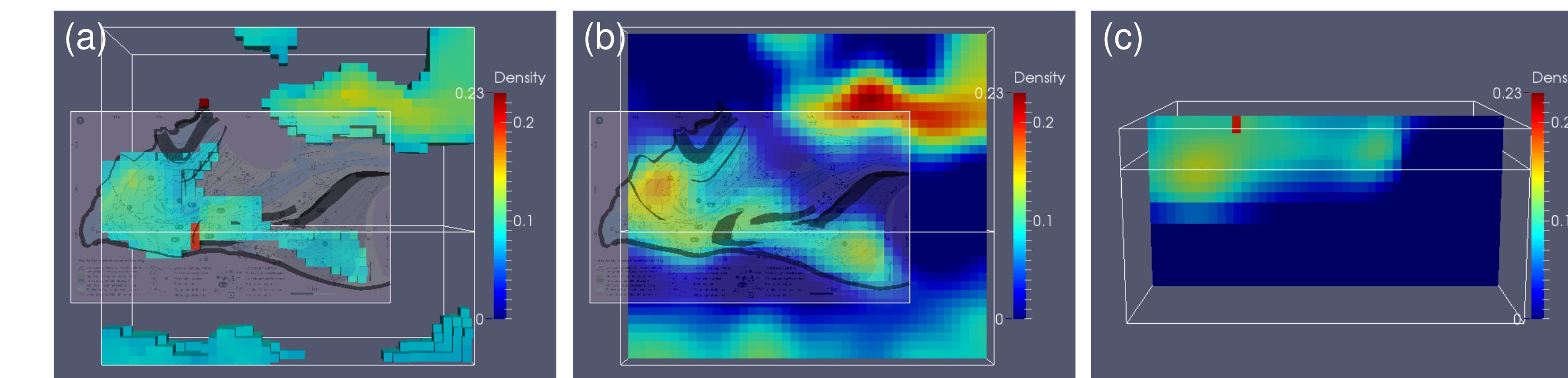


Figure 11 : Density model (g/cc) from cooperative inversion: (a) top view of 0.07 threshold, (b) and (c) as for Fig. 3.

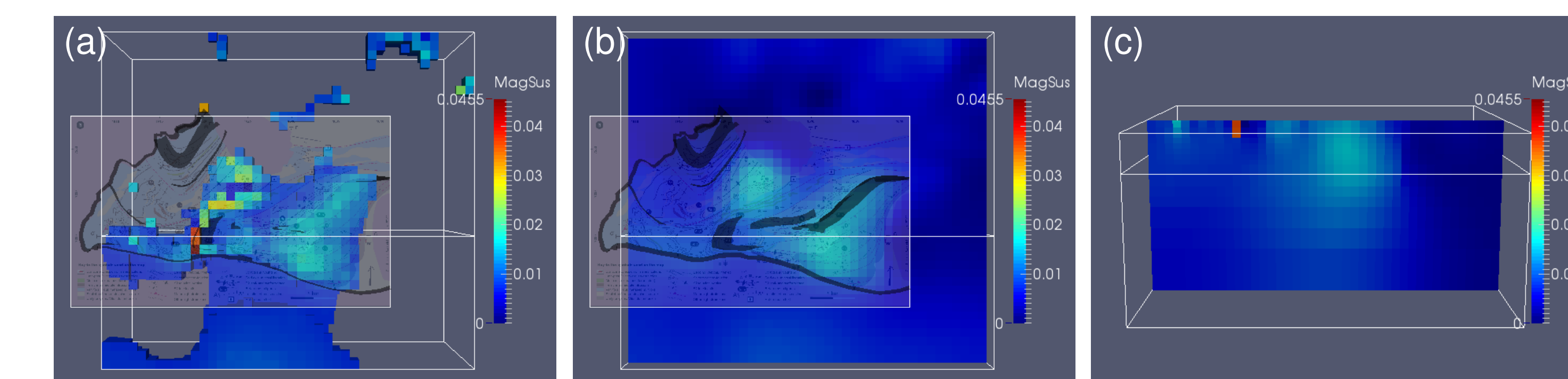


Figure 12 : Magnetic susceptibility model (SI) from cooperative inversion with reduced depth weighting: (a) top view of 0.007 threshold, (b) and (c) as for Fig. 3.

Conclusion and future work

Prior to this work, no attempt had been made to integrate the geophysical and geological data into an integrated 3D Earth model consistent with all information available. For this task, we are considering geologically-constrained joint and cooperative inversion of several different geophysical datasets. Future work will incorporate MT and seismic data into the joint and cooperative inversion strategies. Inversions will also be constrained using interpreted model surfaces. Future joint inversions will need to take higher susceptibilities into account, either by adjusting the coupling or by applying the linear trend only to an appropriate portion of the modelling volume. The failure of the cooperative inversion must be studied and other approaches for structural coupling should be applied. We hope this work will improve our understanding of the geology and reduce 3D model uncertainties.

References

- [1] P. Skyttä, T. Bauer, T. Hermansson, M. Dehghannejad, C. Juhlin, M. García Juanatey, J. Hübner, and P. Weihed. Crustal 3-D geometry of the Kristineberg area (Sweden) with implications on VMS deposits. *Solid Earth*, 4:387–404, 2013.
- [2] Y. Li and D. W. Oldenburg. Separation of regional and residual magnetic field data. *Geophysics*, 63(2):431–439, 1998.
- [3] P. Lelièvre, A. Carter-McAuslan, C. Farquharson, and C. Hurich. Unified geophysical and geological 3D Earth models. *The Leading Edge*, March 2012.
- [4] S. E. Shearer. Three-dimensional inversion of magnetic data in the presence of remanent magnetization. Master's thesis, Colorado School of Mines, Golden, CO, USA, March 2015.
- [5] W. Siripunvaraporn, G. Egbert, Y. Lenbury, and M. Uyeshima. Three-dimensional magnetotelluric inversion: data space method. *Physics of the Earth and Planetary Interiors*, 150:3–14, 2005.
- [6] J. Hübner, M. García Juanatey, A. Malehmir, A. Tryggvason, and L. Pedersen. The upper crustal 3-D resistivity structure of the Kristineberg area, Skellefte district, northern Sweden revealed by magnetotelluric data. *Geophysical Journal International*, 192(2):500–513, 2013.
- [7] P. G. Lelièvre, C. G. Farquharson, and C. A. Hurich. Joint inversion of seismic traveltimes and gravity data on unstructured grids with application to mineral exploration. *Geophysics*, 77(1):K1–K15, 2012.
- [8] T. Günther and C. Rücker. A new joint inversion approach applied to the combined tomography of DC resistivity and seismic refraction data. In *Proceedings of SAGEEP*, Seattle, USA, 2006.